1908–1919 *Nucleic Acids Research, 2019, Vol. 47, No. 4* *Published online 4 January 2019*
doi: 10.1093/nar/gky1310

Rapid formylation of the cellular initiator tRNA population makes a crucial contribution to its exclusive participation at the step of initiation

Riyaz Ahmad Shah[1], Rajagopal Varada[1], Shivjee Sah[1], Sunil Shetty[1], Kuldeep Lahry[1], Sudhir Singh[1] and Umesh Varshney[1,2,*]

[1]Department of Microbiology and Cell Biology, Indian Institute of Science, Bangalore 560012, India and [2]Jawaharlal Nehru Centre for Advanced Scientific Research, Jakkur, Bangalore 560064, India

Received September 05, 2018; Revised December 09, 2018; Editorial Decision December 20, 2018; Accepted December 21, 2018

ABSTRACT

Initiator tRNAs (i-tRNAs) possess highly conserved three consecutive GC base pairs (GC/GC/GC, 3GC pairs) in their anticodon stems. Additionally, in bacteria and eukaryotic organelles, the amino acid attached to i-tRNA is formylated by Fmt to facilitate its targeting to 30S ribosomes. Mutations in GC/GC/GC to UA/CG/AU in i-tRNA$_{CUA/3GC}$ do not affect its formylation. However, the i-tRNA$_{CUA/3GC}$ is non-functional in initiation. Here, we characterised an *Escherichia coli* strain possessing an amber mutation in its *fmt* gene (*fmt*$_{am274}$), which affords initiation with i-tRNA$_{CUA/3GC}$. Replacement of *fmt* with *fmt*$_{am274}$ in the parent strain results in production of truncated Fmt, accumulation of unformylated i-tRNA, and a slow growth phenotype. Introduction of i-tRNA$_{CUA/3GC}$ into the *fmt*$_{am274}$ strain restores accumulation of formylated i-tRNAs and rescues the growth defect of the strain. We show that i-tRNA$_{CUA/3GC}$ causes a low level suppression of am274 in *fmt*$_{am274}$. Low levels of cellular Fmt lead to compromised efficiency of formylation of i-tRNAs, which in turn results in distribution of the charged i-tRNAs between IF2 and EF-Tu allowing the plasmid borne i-tRNA$_{CUA/3GC}$ to function at both the initiation and elongation steps. We show that a speedy formylation of i-tRNA population is crucial for its preferential binding (and preventing other tRNAs) into the P-site.

INTRODUCTION

Transfer RNAs (tRNAs) act as adaptor molecules during the process of translation to bring the cognate amino acid to the site of polypeptide synthesis. The tRNAs can be functionally classified into two types, the initiator and the elongator tRNAs. The initiator tRNAs (i-tRNAs) take part in initiation and, the elongator tRNAs participate at the step of elongation (1). The i-tRNA is special in its direct binding to the ribosomal P-site where its binding is assisted primarily by the initiation factors (IFs). The elongator tRNAs are brought to the A-site by elongation factor Tu (EF-Tu) and then translocated to the P-site by elongation factor G (EF-G). The P-site binding of i-tRNA has been attributed to two of its special features. Firstly, the formylation of the amino acid attached to it facilitates its targeting to the 30S ribosome; and secondly, the presence of the three consecutive G-C base pairs (G29-C41, G30-C40 and G31-C39, or GC/GC/GC or 3GC pairs) in its anticodon stem facilitates its transition through the various stages of initiation (2).

A mismatch at the 1 × 72 position (C1xA72 in *Escherichia coli*) together with the 2–71 and 3–70 bp in the acceptor stem of the i-tRNA are important in its recognition by L-methionyl-tRNA formyltransferase (Fmt) (3,4). Further, the structural studies have revealed that Fmt possesses two domains, an N-terminal domain (NTD) and a C-terminal domain (CTD) joined by a linker. The NTD of Fmt possesses the catalytic site and also recognises the acceptor stem sequences in i-tRNA while the CTD recognises the D-loop and variable loop regions of i-tRNA to enhance its binding. Biochemical studies have shown that a deletion of even 20 amino acids from the C-terminal end results in an inactive protein even though the active site domain is intact (5–8). The formylation of i-tRNA is essential for normal growth of bacteria, and favours initiation with i-tRNA by increasing its affinity to IF2 and facilitates its targeting to the 30S ribosome (9–11). Besides its direct role, the 1 × 72 mismatch is also indirectly important in facilitating binding of the aminoacylated i-tRNA to Fmt, by avoiding its binding to EF-Tu (12). We have earlier shown that a Watson-Crick pair at 1–72 position makes the mutant i-tRNA a poor substrate for Fmt, and allows it to participate in elongation (13). Other studies (12) deduced that when the cellu-

*To whom correspondence should be addressed. Tel: +91 80 22932686; Fax: +91 80 23602697; Email: varshney@iisc.ac.in
Present address: Sunil Shetty, Biozentrum, University of Basel, Basel, Switzerland.

lar levels of Fmt are down regulated even the i-tRNA with its 1 × 72 mismatch could participate at the step of elongation. Also, it was shown that overproduction EF-Tu could lead to misappropriation of i-tRNA at the step of elongation and, overproduction of IF2 could allow initiation to occur with an unformylated tRNA (12). The C1xA72 mismatch is also crucial in protecting the formyl-aminoacyl-i-tRNA from hydrolysis by the peptidyl-tRNA hydrolase (Pth), an enzyme whose primary function is to recycle tRNAs from the peptidyl-tRNAs that fall off the translating ribosomes (14–16).

To study the importance of the various features of i-tRNA *in vivo*, we designed an *in vivo* assay system (17). The assay system allows us to interrogate the importance of the various features of i-tRNA by mutational analysis of the plasmid borne i-tRNA gene without mutating the chromosomally located genes of i-tRNA (*metZWV* and *metY*) in *E. coli*. Subsequently, we developed a genetic screen to investigate mechanism of fidelity of i-tRNA selection on the ribosomal P-site. The genetic screen made use of a mutant i-tRNA (i-tRNA$_{CUA/3GC}$). The mutations in the 3GC pairs render i-tRNA inactive in initiation, in spite of the fact that its aminoacylation and formylation activities were unaffected (17,18). The genetic screen resulted in identification of several strains that allowed the 3GC mutant i-tRNA to participate in initiation. Some of these strains have been characterised earlier (19–21).

Here, we have characterised one more of these strains, called B2 (19). The study shows that an amber mutation in *fmt* at amino acid position 274 (*fmt*$_{am274}$) allows this strain to initiate with i-tRNA$_{CUA/3GC}$. Also, under the limiting Fmt levels, even a tRNA with a mismatch at 1 × 72 position participates in elongation. The study shows that not just the formylation of i-tRNA but a swift formylation of the cellular i-tRNA population is crucial to ensure fidelity of translation initiation.

MATERIALS AND METHODS

Chemicals, media, enzymes and radioisotopes

Chemicals were obtained from Sigma (USA), GE Healthcare or Qualigens (India). Media components were procured from BD Biosciences (Difco™, USA). The enzymes for various DNA manipulations were obtained from New England Biolabs (USA), Fermentas (USA) or Takara (Japan). Radioisotopes were from Board of Radiation and Isotope Technology (BRIT, India) and American Radiolabeled Chemicals Co. Pvt Ltd (USA). DNA oligomers were from Sigma-Aldrich (India) or Macrogen (South Korea).

Strains, plasmids, DNA oligomers, and growth conditions

The bacterial strains, plasmids and the DNA oligomers used are listed in Supplementary Tables S1, S2 and S3, respectively. *Escherichia coli* strains were grown in Luria-Bertani (LB) or LB-agar plates containing 1.8% bacto-agar (Difco™). Unless mentioned otherwise, media were supplemented with ampicillin (Amp, 100 μg/ml), chloramphenicol (Cm, 30 μg/ml), kanamycin (Kan, 25 μg/ml) or tetracycline (Tet, 5 μg/ml) as required.

Growth analyses

Bacterial growth was monitored by plate assays or growth curve analyses. For plate assays, overnight grown cultures were streaked on LB agar or MacConkey agar plates containing desired antibiotics and incubated at the desired temperatures for various times and imaged using a gel doc (Alpha Imager, Alpha Innotech). For growth curve analyses, four independent colonies of each strain were inoculated and grown overnight in LB with the desired antibiotic(s) and temperatures until they reached saturation. The saturated culture was serially diluted a thousand fold (10^{-3} dilution) in LB or minimal media, and 200 μl aliquots were grown in honeycomb plates in Bioscreen C growth reader. $OD_{600\ nm}$, at desired temperature, was measured every hour. Standard mean $OD_{600\ nm}$ values for each strain were plotted against time using GraphPad Prism software.

Isolation, characterization and genetic mapping of B2 suppressor strain

The isolation of *E. coli* B2 suppressor has been detailed earlier (19). Whole genome sequencing (WGS) of B2 was performed at Scigenom, Cochin, Kerala, India. The WGS was compared to *E. coli* K-12 reference genome (RefSeq NC_000913) to identify unique SNPs in B2. Mapping of the suppressor mutation was done by P1 mediated transductions using *E. coli* CAG strains harboring Tet^R marker at known loci (from Coli Genome Stock Centre, CGSC).

Cloning of wild type *fmt* gene

Escherichia coli fmt gene (wild type) was PCR amplified using Fmt-Fp and Fmt-Rp primers and *Pfu* DNA polymerase. The reactions were heated at 94°C for 5 min followed by 35 cycles of incubations at 94°C 1 min, 55°C 40 s, 72°C 2 min and a final extension of 72°C 10 min. The amplicon was digested with NdeI and HindIII, ligated to pACDH-NdeI at the same sites to generate pACDH*fmt* or p*fmt*, and verified by DNA sequencing.

Generation of *fmt* deleted strain

P1 lysate was generated on TG1Δ*fmt*::*kan* strain (22) and transduced into the KL16 strain. The transductants were selected on LB agar containing Kan at 37°C. The *fmt* deletion strain was identified by its slow growth phenotype and confirmed by PCR and DNA sequencing.

Generation of *fmt* C-terminal deletion strains

Various C-terminal *fmt* deletion strains were generated according to Datsenko and Wanner (23). Briefly, *kan*^{R} cassette from pKD4 was amplified using forward primers designed in the C-terminal of *fmt* (depending on the strain to be generated) and a common reverse primer (FmtFRT new Rp). The amplicons were purified from agarose gel and electroporated into KL16/pKD46. The colonies were selected on LB agar containing Kan and the mutants were confirmed by diagnostic PCR using MTF-F2 and MTF-R3 primers and DNA sequencing. Similarly, a strain KL16Δ0*fmt*:*kan* with wild type *fmt* linked to the *kan*^{R} cassette was generated

using the forward primer (FmtΔ0FRT Fp) and a common reverse primer (FmtFRT New Rp).

Generation of KL16*fmt*$_{am274}$:*kan* and CA274 *fmt*$_{am274}$:*kan* strain

The KL16*fmt*$_{am274}$:*kan* strain was generated by pKD46 mediated recombination (23). We first generated KL16Δ0*fmt*:*kan* with wild type *fmt* linked to *kan*^{R} cassette. Using a forward primer (Fmt 274TAG Fp) containing the suppressor mutation and a reverse primer (FmtFRT new Rp), the C-terminus of *fmt* along with the *kan*^{R} cassette was PCR amplified from KL16Δ0*fmt*:*kan* DNA. The amplicon was electroporated into KL16/pKD46 to obtain KL16*fmt*$_{am274}$:*kan*. To generate CA274*fmt*$_{am274}$:*kan*, P1 phage lysate raised on KL16*fmt*$_{am274}$:*kan* was transduced into CA274 strain, and the transductants were selected on LB agar containing Kan. The strain was confirmed by colony PCR using MTF-F3 and MTF-R3 primers and the amplicon sequencing.

Generation of FLAG tagged strains

FLAG tagged *fmt* strain was generated as before (24). Briefly, the FLAG tag along with *kan*^{R} cassette was PCR amplified from pSUB11 using forward (Fmt 3XFLAG_Fp or FmtD42 3XFLAG_Fp) that has 5′ end homology with C-terminal of *fmt* (depending on the strain to be generated) and 3′ end homology with pSUB11 and a reverse primer (Fmt 3XFLAG_Rp) with homology downstream of *fmt* and also pSUB11 plasmid. The PCR product was purified and electroporated into KL16/pKD46. The colonies were selected on LB agar containing Kan and the strain identity was checked by PCR using MTF-F3 and MTF-R3 and verified by DNA sequencing. Similarly, the KL16*fmt*$_{am274}$ 3XFLAG strain was generated using a forward primer (Fmt 274TAG Fp) that carried the am274 mutation in it and reverse primer (FmtFRT new Rp) and genomic DNA of KL16*fmt* 3XFLAG strain as template, to amplify the C-terminal region along with 3XFLAG and *kan*^{R} cassette and confirmed by PCR and DNA sequencing.

Isolation of tRNAs

Total tRNA was prepared from various strains under cold and acidic conditions to preserve the ester linkage between the amino acid and the tRNA (13). For preparations under neutral conditions, the cells were resuspended in 1× TE (10 mM Tris–HCl pH 8.0, 1 mM Na_2EDTA) and extracted with water saturated phenol. Rest of the procedure was the same as before (13).

Acid urea gels and northern blotting

The tRNA samples (2–4 μl) prepared under acidic condition were either not treated or treated with 10 mM $CuSO_4$ in 100 mM Tris–HCl (pH 8.0) to deacylate aminoacylated tRNA (formylated tRNA is resistant) or with 100 mM Tris–HCl (pH 9.0) to deacylate both the formylaminoacyl- and the aminoacyl- forms of tRNA (25,26). The samples were mixed with equal volumes of acid-urea dye (0.1 M sodium acetate (pH 5.0), 10 mM Na_2EDTA, 8 M urea, 0.05% bromophenol blue and 0.05% xylene cyanol FF), separated on 6.5% polyacrylamide gel containing 8 M urea and 0.1 M sodium acetate (pH 5.0 buffer), and electroblotted onto a nytran membrane at 15 V for 20 min (13). The tRNAs were fixed onto the membrane by UV cross linking at 120 mJ/cm^2 (CL1000-UV products). The membranes were blocked using pre-hybridization buffer containing yeast total RNA and Denhardt's solution (1% BSA, 1% ficoll, 1% polyvinylpyrrolidone 40), and hybridised with 5′-^{32}P end-labelled DNA oligomers to detect tRNAs. Various probes such as Met33 (complementary to positions 25–39 of wild type i-tRNA), 3GCam probe (complementary to i-tRNA *met* $Y_{CUA/3GC}$ positions 25–40), met elongator (complementary to tRNA^{Met} D loop positions 2–27) were used. The blots were exposed to phosphor-imager screen for analysis on Bio Image analyser (FLA5100, Fuji Film).

Analysis on native gels

Total tRNAs (prepared at neutral pH) were separated on 15% native PAGE (using 1× TBE, pH 8.0) at room temperature till xylene cyanol FF reached the bottom, electroblotted onto a nytran membrane, and analyzed by northern blotting using radiolabelled DNA probes as above.

Preparation of cell-free extracts and chloramphenicol acetyltransferase (CAT) assays

Four replicates of each of the *E. coli* strains were grown in 3 ml LB with required antibiotics at 37°C to log phase ($O.D._{600}$ ∼ 0.6–0.7), processed as before (19) and stored in 10 mM Tris–HCl pH 8.0, 5 mM β-mercaptoethanol, 100 mM NaCl and 40% glycerol (v/v) at −20°C. The protein contents of the extract were quantified by Bradford's assay (27). Reactions (30 μl) containing 500 mM Tris–HCl, pH 8.0, 150 μM chloramphenicol, 0.025 μCi (430 pmoles) [^{14}C]-Cm (specific activity 57.8 mCi mmol^{-1}; Perkin Elmer), 432 μM acetyl-CoA and varying amounts of total cell protein (depending on the strain) were set up for 20 min at 37°C and stopped by addition of 300 μl ethyl acetate followed by thorough vortexing and centrifugation at 15, 400 g for 2 min. Top 200 μl volume was transferred to fresh microcentrifuge tube, vacuum dried and dissolved in 10 μl ethyl acetate. The samples were spotted on a silica gel 60 plate (Merck) and thin layer chromatography (TLC) was performed using chloroform:methanol (95:5) as mobile phase. The TLC plate was exposed to phosphor-imager screen and scanned using a Bio Image Analyzer (FLA5100, Fuji). The pixel values were quantitated in the spots corresponding to substrate and products using Multi Gauge V2.3 software. CAT activities were calculated as pmols of chloramphenicol converted to its acetylated forms per μg of total protein.

β-Galactosidase assay

β-Galactosidase assay was performed using the Miller's protocol (28). Five replicates of each strain were grown overnight at 37°C in LB liquid media, sub-cultured into 3 ml fresh LB using 1% inoculum, grown at 37°C till 0.4

$OD_{600\,nm}$, induced with 0.5 mM IPTG and harvested at log phase (0.6 $OD_{600\,nm}$). The cell pellet was resuspended in Z-buffer (60 mM Na_2HPO_4, 40 mM NaH_2PO_4, 10 mM KCl, 0.1 mM $MgSO_4$, 50 mM β-mercaptoethanol, pH 7.4). Lysis was done by adding 10 μl of lysozyme (1 mg/ml) followed by addition of 5 μl of DNase I (1 mg/ml) to degrade DNA. The lysate was assayed for β-galactosidase activity at 37°C using ortho-nitrophenyl β-galactoside (ONPG, 4 mg /ml) as substrate. The reaction was carried out for different times until it developed yellow color and stopped by adding 500 μl of 1 M Na_2CO_3. The time of reaction was noted for each sample. The product intensity was estimated at $OD_{420\,nm}$ and β-galactosidase activity was calculated in Miller units using Miller's formula.

In vitro formylation assay

Total tRNA under native conditions was prepared from KL16Δ*fmt* strain overexpressing *metY* to get deacylated tRNA. The deacylated tRNA was charged with methionine using *E. coli* MetRS. Briefly, 10 μl (170 μg) of tRNA was incubated with 180 ng of MetRS for 1 h in aminoacylation buffer (50 mM HEPES buffer, pH 7.3, 25 mM KCl, 2 mM DTT, 10 mM $MgCl_2$, 1 mM ATP, 0.1% BSA and 2 mM methionine). The methionine charged tRNA was incubated with 10-CHO-THF (450 μM) and total cell proteins of KL16/ $pCAT_{am1}metY_{CUA/3GC}$ (8 μg) or KL16fmt_{am274}/$pCAT_{am1}metY_{CUA/3GC}$ (80 μg) strains for different time intervals in 2× diluted aminoacylation buffer. The samples were then mixed with equal volumes of acid-urea dye (0.1 M sodium acetate pH 5.0, 10 mM Na_2EDTA, 8 M urea, 0.05% bromophenol blue and 0.05% xylene cyanol FF), and resolved on 6.5% polyacrylamide gel containing 8 M urea and 0.1 M sodium acetate (pH 5.0). The gel was electrophoresed at 4°C till the bromophenol blue reached the bottom of the gel, electroblotted onto a nytran membrane at 15 V for 20 min and analysed for formylation by northern blotting using probes specific to i-tRNA.

Immunoblotting with anti-FLAG antibodies

Total cell proteins prepared from various strains were separated on 12% SDS-PAGE, and transferred onto polyvinylidenedifluoride (PVDF) membrane in a BioRad semi-dry trans-blot apparatus at 15 V for 1 h. The membrane was blocked with 5% skimmed milk in 1× TBST [20 mM Tris–HCl, pH 7.5, 0.9% NaCl and Tween 20 (0.2% v/v)] by keeping for 3–4 h on a rocker at room temperature, and washes thrice for 10 min each with 1× TBST. Mouse anti-FLAG primary antibody (1:8000) was added and incubated for 3–5 h at room temperature on rocker, followed by three 10 min washes with 1× TBST. The membrane was incubated with secondary antibody (1:5000 α-mouse IgG-HRP, Genei) for 2–3 h, and followed by three successive washes of 10 min each with 1× TBST. Blot was developed using ECL reagent (Millipore) and scanned in a Chem Doc (GE), and quantified by Image-Quant and Multi Gauge V2.3 software.

IF2 and EF-Tu pull down assay

IF2 pull down was performed from wild type KL16 or KL16fmt_{am274} cells containing $pCAT_{am1}metY_{CUA/3GC}$ plasmid and overexpressing His-tagged IF2 from pACDH clone. About 300 ml culture was grown to log phase (0.6 $OD_{600\,nm}$) at 37°C without any induction. The culture was chilled on ice for 5 min. All further steps were performed at 4°C. The cells were harvested, washed with buffer A (20 mM Tris–HCl, pH 8.5, 2 mM β -mercaptoethanol, 500 mM NaCl, 10 mM imidazole and 1 mM GTP) and then resuspended in 4 ml of buffer A. Lysozyme (100 μl of 40 mg/ml) prepared in 20 mM Tris–HCl pH 8.8 and 1 mM GTP was used to lyse the cells. The lysate was incubated on ice for 1 h and further lysis was carried out by freeze thaw cycles in liquid nitrogen and ice. DNase I (200 μl, 1 mg/ml) was added to the lysate and kept on ice for 20 min, and centrifuged at 15, 400 g for 20 min at 4°C to remove the cell debris and cleared supernatant was incubated with 100 μl Ni-NTA agarose beads (Qiagen) for 2 h at 4°C. Before incubation, Ni-NTA beads were pre-equilibrated with buffer A. The beads were harvested and washed 2–3 times with 1 ml buffer A. Bound protein was eluted with 300 μl of buffer A containing 500 mM imidazole. Eluent (20 μl) was electrophoresed on 12% SDS-PAGE to visualize the pulled down proteins. For tRNA visualization, 50 μl of the eluted fraction was resolved on 15% native PAGE, transferred to nytran membrane and analysed by northern blotting using probes specific i-tRNA such as Met33 (complementary to positions 25–39 of wild type i-tRNA), 3GCam probe (complementary to $i\text{-}tRNA_{CUA/3GC}$ positions 25–40), met elongator (complementary to $tRNA^{Met}$ D loop positions 2–27). The blots were exposed to phosphor-imager screen and analyzed on BioImage Analyzer (FLA5100, Fuji Film). For EF-Tu pull down experiment, genomic *tuf*B locus encoding EF-Tu was His tagged by standard genetic technique in KL16 or KL16fmt_{am274} strain. The His-tagged EF-Tu strains were used for pull downs as mentioned above.

RESULTS

In vivo assay system and the validation of the B2 suppressor strain

The plasmid $pCAT_{am1}metY_{CUA}$ contains a $metY_{CUA}$ gene encoding i-tRNA with CUA anticodon ($i\text{-}tRNA_{CUA}$), and a chloramphenicol acetyltransferase (CAT) gene reporter with UAG start codon (CAT_{am1}). When introduced in *E. coli*, it confers chloramphenicol (Cm) resistance to the host (Figure 1A, i; and 1B, sector 2). As shown earlier (17), in this plasmid borne assay system, $i\text{-}tRNA_{CUA}$ is aminoacylated by GlnRS to produce $Gln\text{-}i\text{-}tRNA_{CUA}$ and formylated by Fmt to produce $fGln\text{-}i\text{-}tRNA_{CUA}$ which initiates from the UAG start codon of the CAT_{am1} reporter mRNA to produce CAT protein. Mutations in the highly conserved 3GC pairs in the anticodon stem of $i\text{-}tRNA_{CUA}$ to those corresponding to the anticodon stem sequence of elongator species of methionine tRNA render the i-tRNA mutant ($i\text{-}tRNA_{CUA/3GC}$) inactive in initiation and lack of any detectable Cm resistance to the host by the plasmid, $pCAT_{am1}metY_{CUA/3GC}$ (Figure 1A, ii; and 1B, sector 3) even though the tRNA accumulates in fully formylated form (18). Earlier (19), we isolated a number of suppressor strains of *E. coli* which allow initiation to occur with $i\text{-}tRNA_{CUA/3GC}$.

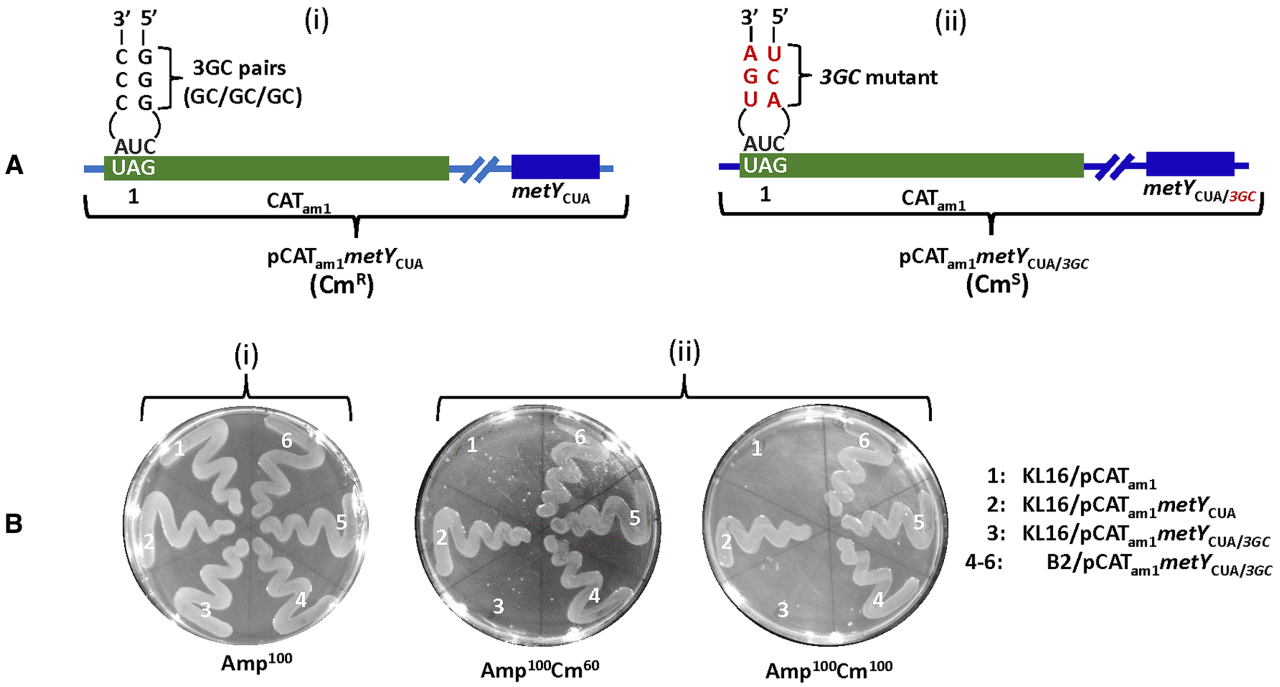

Figure 1. Assay system and initiation activity. (**A**, i) Schematic representation of pCAT$_{am1}$*met Y*$_{CUA}$ harboring CAT$_{am1}$ and *met Y*$_{CUA}$ genes. The three GC base pairs in the stem of the anticodon stem loop of the i-tRNA$_{CUA}$ are shown. (**A**, ii) Schematic representation of pCAT$_{am1}$*met Y*$_{CUA/3GC}$ derived from pCAT$_{am1}$*met Y*$_{CUA}$ wherein the three GC base pairs were mutated to those found in *E. coli* tRNA^{Met}. (**B**) Growth of the *E. coli* strains at 37°C on LB agar plate containing (i) Amp 100 μg/ml; (ii) Amp 100 μg/ml and chloramphenicol (Cm) 60 or 100 μg/ml as indicated. Overnight cultures of *E. coli* KL16 parent strain containing pCAT$_{am1}$ (sectors 1), pCAT$_{am1}$*met Y*$_{CUA}$ (sectors 2), pCAT$_{am1}$*met Y*$_{CUA/3GC}$ (sectors 3) or *E. coli* B2 suppressor strain containing pCAT$_{am1}$*met Y*$_{CUA/3GC}$ (sectors 4–6) were streaked and incubated at 37°C for ∼18 h.

This investigation is focused on one of the previously uncharacterised suppressors named, B2. Unlike the parent strain KL16 (harboring pCAT$_{am1}$*met Y*$_{CUA/3GC}$), the B2 strain (harboring pCAT$_{am1}$ *met Y*$_{CUA/3GC}$), confers Cm resistance (Figure 1B, ii, compare sector 3 with sectors 4–6). As a control, both the strains grow on Amp containing LB agar plate (Figure 1B, i sectors 1–6). Further validation of the B2 strain involved CAT activity assays using the cell-free extracts (Supplementary Figure S1A). While the growth analysis of B2 revealed only a slightly increased lag phase (compared to the KL16 parent) in the rich media (LB), its growth was significantly affected in M9 minimal medium (Supplementary Figure S1B and S1C).

Identification and characterization of the suppressor mutation

To identify the mutation in B2, which afforded initiation with the i-tRNA$_{CUA/3GC}$, we performed whole genome sequencing (WGS) of the strain, which identified 306 SNPs when compared with the reference genome of *E. coli* K-12 (RefSeq NC_000913). Elimination of SNPs common to other suppressor strains (unpublished), and the synonymous mutations, limited the unique SNPs in the B2 strain to 60. Candidate gene approach suggested that the appearance of a C to T transition at nucleotide position 820 corresponding to a change of Gln (CAG) to an amber (UAG) codon (referred to as *fmt*$_{am274}$) in the ORF of *fmt* as a putative candidate (Figure 2A). The *fmt*$_{am274}$ allele would be expected to code for an Fmt with truncation of 42 amino acids from the C-terminal end (Figure 2B). Genetic mapping using P1 mediated transductional crosses between a CAG12071 strain harboring Tet^R marker at 73.88′ locus and the B2, and the KL16 parent confirmed that *fmt*$_{am274}$ is indeed responsible for the suppressor phenotype. Consistent with the results of genetic mapping, introduction of the wild type *fmt* on a plasmid (p*fmt*) in B2 resulted in the loss of initiation with i-tRNA$_{CUA/3GC}$ and loss of its Cm^R (Figure 2C, ii compare sectors 3, 4 with sectors 5, 6). CAT assays also confirmed that the occurrence of amber mutation in *fmt* is responsible for initiation with i-tRNA$_{CUA/3GC}$ (Figure 2D, compare blue and green bars). The growth defect of B2 strain was also rescued upon its complementation with the wild type *fmt* (Supplementary Figure S2).

Status of i-tRNAs in B2

It was earlier shown that a deletion of 20 amino acids from its C-terminal end rendered Fmt inactive (6). However, when we analysed the steady state accumulation of the cellular i-tRNAs on acid urea gels, the i-tRNAs (both the chromosomally encoded i-tRNA, and the plasmid encoded i-tRNA$_{CUA/3GC}$) accumulated in formylated form both in the KL16 parent and its B2 derivative (Figure 3A and Supplementary Figure S3A). Generation of a KL16 strain (KL16*fmt*Δ42) harboring *fmt* with deletion of sequences downstream of the amber mutation at position 274 resulted in accumulation of i-tRNA in aminoacylated (but not formylated) form as in *E. coli* deleted for full length *fmt* (KL16Δ*fmt*) (Figure 3A). Consistent with the *in vitro* exper-

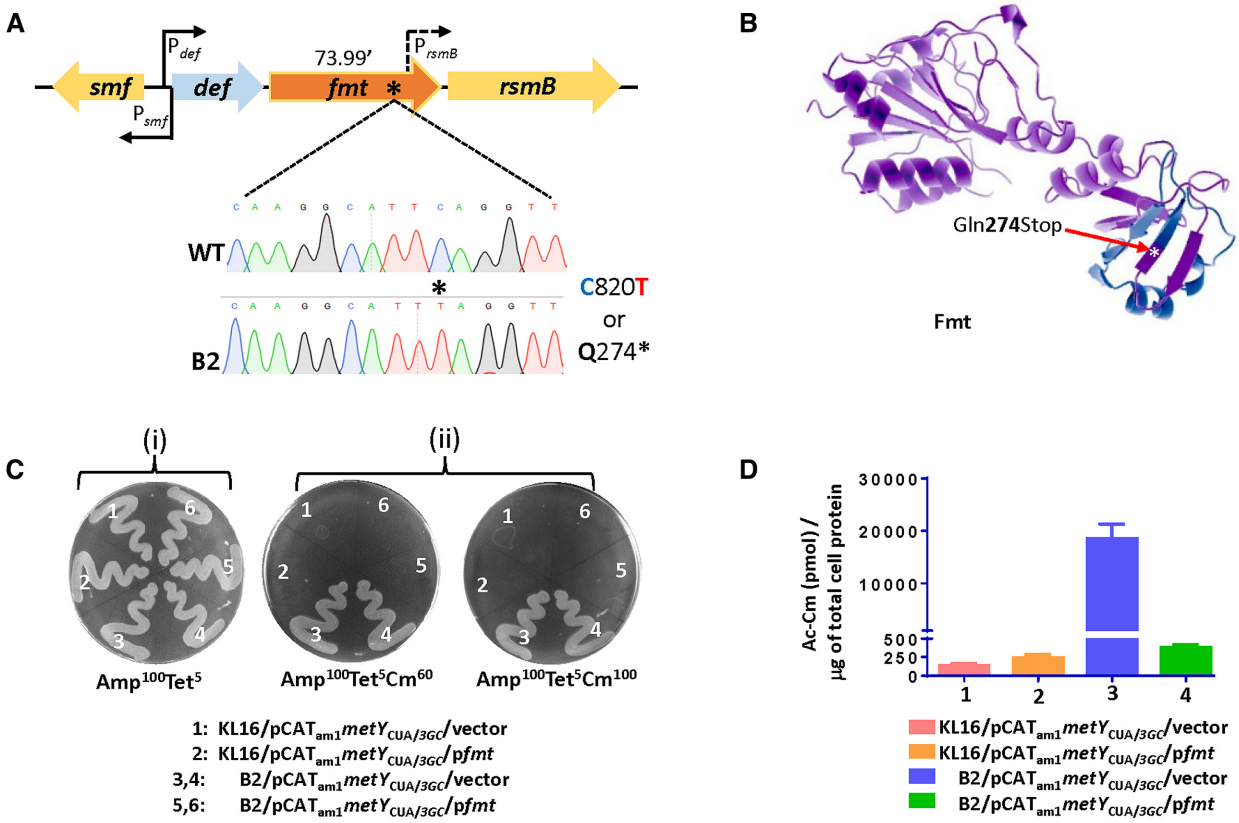

Figure 2. Characterization of B2 suppressor strain (**A**) Schematic representation of *fmt* gene locus. Colored arrows indicates direction of each gene, black arrows indicate promoters and the asterisk '*' indicates the position of the mutation in the *fmt* gene. Relevant part of *fmt is* zoomed-in to show the C to T mutation in B2 *fmt* at position 820 leading to change of CAG codon (Gln) to TAG codon (am274). (**B**) Structure of Fmt prepared from PDB entry 1FMT (5) using PyMOL. Fmt is represented by pink ribbon structure with C-terminal 42 amino acids shown in blue ribbon. The position of Gln274am change (marked by asterisk in the structure) is indicated by the red arrow. (**C**) Growth of indicated *E. coli* strains at 37°C on LB agar plate containing (i) Amp 100 μg/ml, Tet 5 μg/ml; (ii) Amp 100 μg/ml, Tet 5 μg/ml and Cm 60 or 100 μg/ml as indicated. Overnight cultures of *E. coli* KL16/pCAT$_{am1}$*metY*$_{CUA}$ containing a compatible vector (sectors 1) or p*fmt* (sectors 2) and *E. coli* B2/pCAT$_{am1}$*metY*$_{CUA}$ suppressor strain containing vector (sectors 3, 4), or p*fmt* (sectors 5, 6), were streaked and incubated at 37°C for ∼18 h (**D**) Initiation with i-tRNA$_{CUA/3GC}$ as assayed by CAT activity in cell-free extracts of *E. coli* KL16/pCAT$_{am1}$*metY*$_{CUA/3GC}$ and B2/pCAT$_{am1}$*metY*$_{CUA/3GC}$ strains harboring vector (bars 1 and 3, respectively) or p*fmt* (bars 2 and 4, respectively). The CAT activities are plotted as acetylated (Ac) Cm produced per μg of total protein in 20 min at 37°C.

iments (6), we observed that even under *in vivo* conditions, a deletion of 20 or more (e.g. 42 or 80) amino acids from the C-terminal end of Fmt abolished its formylation activity (Supplementary Figure S3C). Furthermore, contrary to the B2 strain, both the KL16*fmt*Δ42 and the KL16Δ*fmt* showed a severe decrease in their growth rate (Supplementary Figure S3B), suggesting a possibility of expression of functional Fmt in B2.

fmt $_{am274}$ mutation in B2 is suppressed by i-tRNA$_{CUA/3GC}$

Accumulation of i-tRNAs in formylated form, and the lack of severe growth defect in B2 suggested a read through of the amber codon in *fmt*$_{am274}$. Hence, we generated a KL16 strain with a point mutation (C820T) in *fmt* (KL16*fmt*$_{am274}$:*kan*) similar to that found in B2 but linked it with *kan* marker for selection and transfer between the strains. Like the KL16Δ*fmt* strain, the KL16 *fmt*$_{am274}$:*kan* strain (harboring an empty vector) also showed a severely retarded growth phenotype compared to parent KL16 and the B2 strains (Figure 3C). And, the i-tRNA accumulated in aminoacylated (not formylated) form (Figure 3B, lane 3). However, introduction of pCAT$_{am1}$*metY*$_{CUA/3GC}$ into the KL16 *fmt*$_{am274}$:*kan* strain, rescued its growth defect (Figure 3C, compare curves 4 and 5). Plate assays on chloramphenicol showed that the *fmt*$_{am274}$ allele afforded initiation with i-tRNA$_{CUA/3GC}$ (Supplementary Figure S4). Status of the accumulated i-tRNAs in the cell also changed to that of formylated form (Figure 3B, lanes 5 and 6), indicating that the i-tRNA$_{CUA/3GC}$ with CxA mismatch at 1 × 72 position (the only tRNA in the cell with CUA anticodon) participated at in elongation to read through the amber codon at 274 (am274) in Fmt. Interestingly, as the i-tRNA$_{CUA/3GC}$, is aminoacylated with Gln, read through of the am274 codon would produce wild type Fmt from *fmt*$_{am274}$.

The i-tRNA$_{CUA/3GC}$ mediated read through of the am274 codon in *fmt*$_{am274}$ produces a low level of full length Fmt

To detect Fmt expression in various strains, a 3X FLAG tag was introduced at the end of the ORFs of the *fmt* genes in the parent KL16 (*fmt*-3XFLAG:*kan*) and the KL16*fmt*$_{am274}$ (*fmt*$_{am274}$-3XFLAG:*kan*) strains using pSUB11/pKD46 mediated recombination (24). Im-

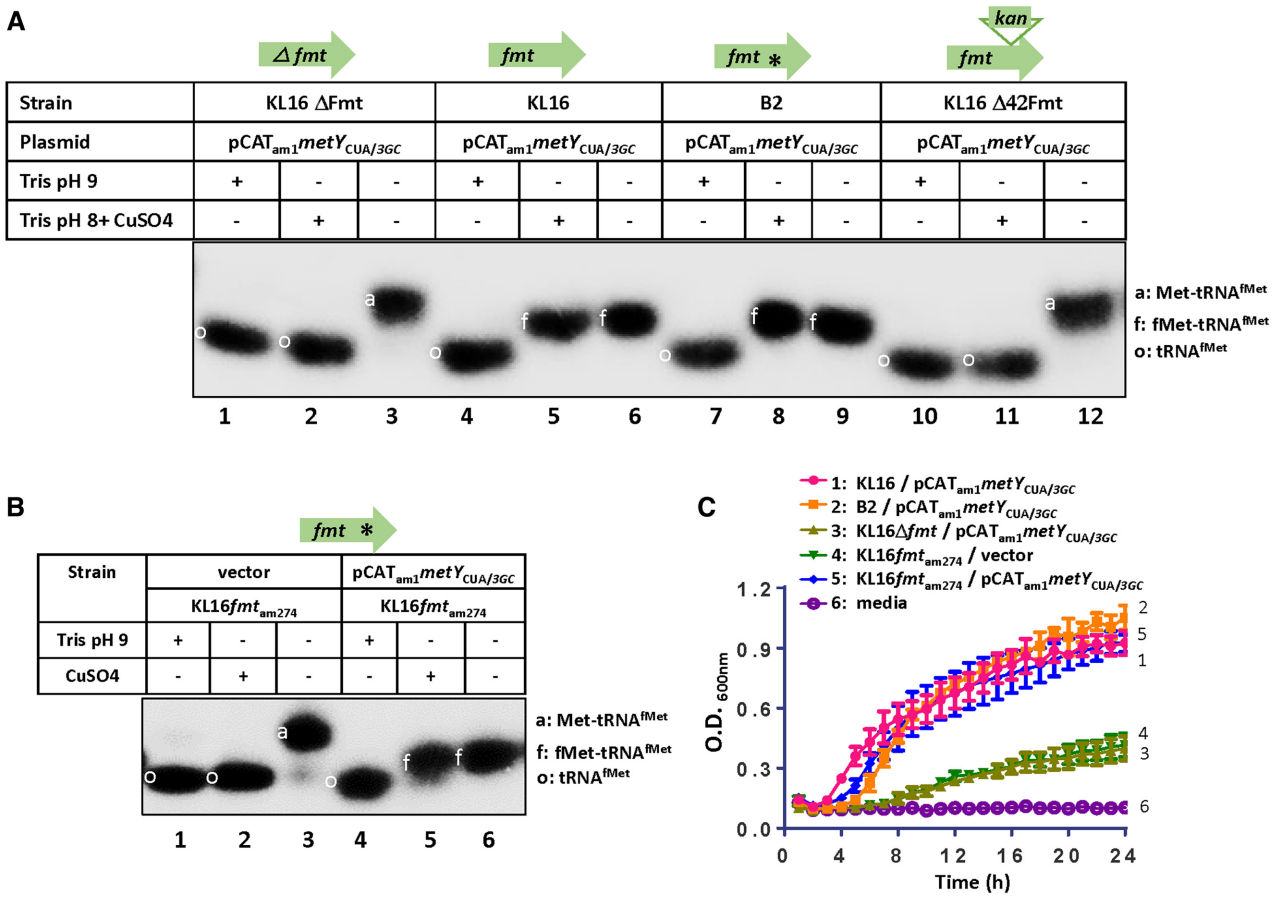

Figure 3. Formylation of i-tRNA, and growth of *E. coli* strains. (**A**) Aminoacylation and formylation of i-tRNA in different *fmt* strains. Total tRNA was prepared under acidic conditions, separated by acid urea PAGE, transferred onto nytran membrane and probed with i-tRNA specific probes. For each strain, the tRNA was also deacylated using Tris–HCl, pH 9 (lanes 1, 4, 7 and 10), or treated with $CuSO_4$ in the presence Tris-HCl, pH 8 (lanes 2, 5, 8 and 11) to detect formylated form. Samples from KL16Δ*fmt*, KL16 parent strain, B2 strain, and KL16Δ42*fmt* are shown in lanes 1–3, 4–6, 7–9 and 10–12, respectively. (**B**) Analysis of *in vivo* status of i-tRNAs from KL16*fmt*$_{am274}$ in the absence (lanes 1–3) or presence of p*metY*$_{CUA/3GC}$ (lanes 4–6). (**C**) Growth of *E. coli* strains at 37°C in LB broth containing Amp. The parent KL16 (pink line, marked 1), B2 (orange line, marked 2), KL16Δ*fmt* (light green line, marked 3), KL16*fmt*$_{am274}$ (green line, marked 4) and KL16*fmt*$_{am274}$ strain harboring p*metY*$_{CUA/3GC}$ (blue line, marked 5) strains are as shown.

munoblot analysis of the cell-free extracts using anti-FLAG antibodies showed no detectable Fmt in KL16*fmt*$_{am274}$ (Figure 4A i and ii, lane/bar 5). However, introduction of i-tRNA$_{CUA/3GC}$ resulted in production of low levels of full length Fmt in KL16*fmt*$_{am274}$ (Figure 4A i and ii, lane/bar 6). Wild type Fmt in KL16 *fmt*-3X FLAG:*kan* strain (Figure 4A i and ii, lanes/bars 1 and 2) and truncated Fmt in KL16 *fmt*Δ42-3X FLAG:*kan* strain (Figure 4A i and ii, lanes/bars 3 and 4) could also be detected irrespective of the i-tRNA$_{CUA/3GC}$ presence. As a control, in the KL16*fmt*$_{am274}$ strain harboring i-tRNA$_{CUA/3GC}$ but lacking a FLAG tag at its *fmt* locus, we did not detect any Fmt (Figure 4A, lane/bar 7).

Our *in vivo* analyses using acid urea gels showed accumulation of i-tRNA in formylated form in B2. As this analysis detects the steady state accumulation of formylated/aminoacylated tRNAs, it does not reveal the kinetics of formylation of the tRNA population. Thus, to assess formylation kinetics of methionine charged i-tRNA (chromosomally encoded), we used cell-free extracts of the parent KL16 or the KL16*fmt*$_{am274}$ strains harboring pCAT$_{am1}$*metY*$_{CUA/3GC}$, in the presence of 10-formyl THF. Use of cell-free extract of KL16*fmt*$_{am274}$ showed a highly compromised formylation activity (~45-fold) in B2 (Figure 4B i and ii). Thus, although the acid urea gel *fmt*$_{am274}$ shows accumulation of i-tRNA in fully formylated form, the kinetics of formylation, at a given time, must be compromised even *in vivo* due to the diminished production of Fmt. Thus, to obtain *in vivo* evidence for compromised formylation of i-tRNA, we decided to directly freeze the actively growing culture in ethanol (pre-chilled at −80°C), and followed it by a rapid step of treatment of the cells with acidic phenol. We could detect nearly 30–40% of i-tRNAs in aminoacylated but non-formylated state in the strain with *fmt*$_{am274}$ mutation (Supplementary Figure S5). This compromised efficiency of formylation might result in transient availability of a finite population of the unformylated i-tRNA molecules which in turn bind to EF-Tu and participate in elongation.

A compromised efficiency of formylation allows participation of i-tRNA$_{CUA/3GC}$ in elongation

Characterisation of B2 suggests that the mutation in *fmt* (*fmt*$_{am274}$) allows i-tRNA$_{CUA/3GC}$ to participate both at the

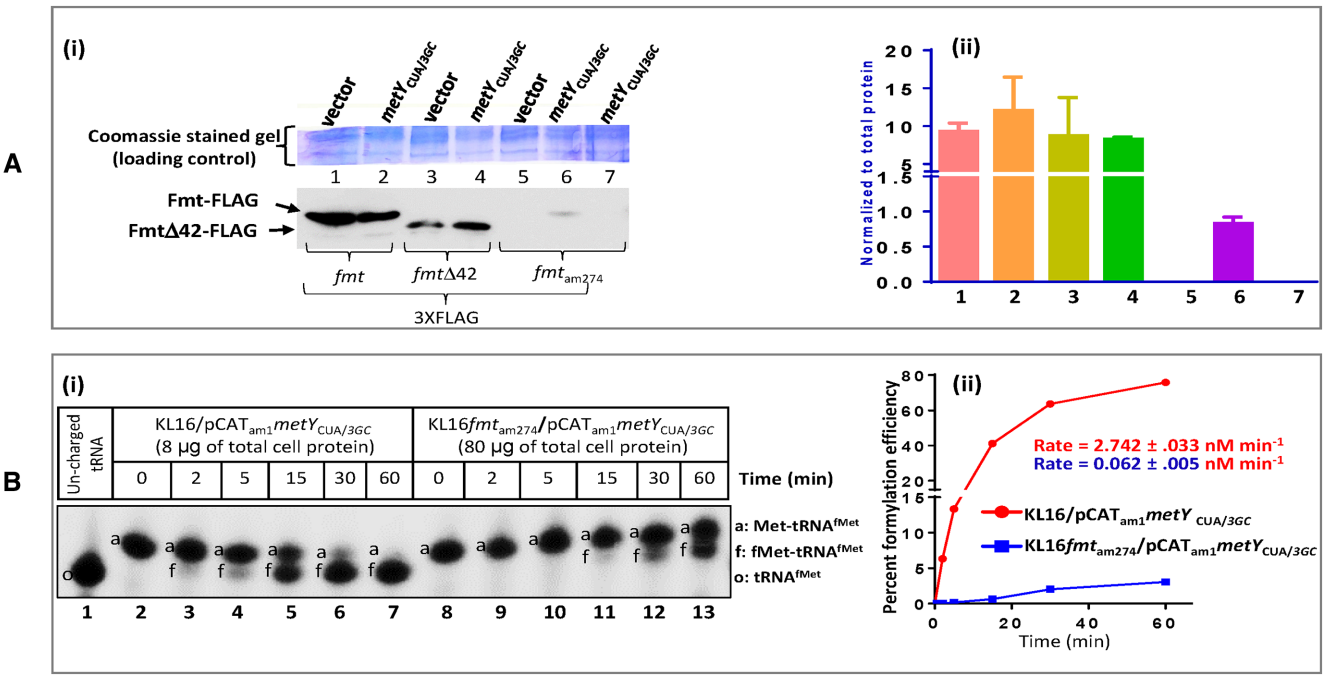

Figure 4. Read through of fmt_{am274} and formylation efficiency. (**A**, i) Immunoblotting to assess Fmt levels in different *E. coli* strains. (**A**, ii) Quantification of immunoblot normalised to total protein. The 3X Flag tagged Fmt or Δ42Fmt bands are as indicated. Lane 1/bar 1 and lane 2/bar 2 show KL16 harboring vector or $pCAT_{am1}metY_{CUA/3GC}$, respectively. Lane 3/bar 3 and lane 4/bar 4 show KL16Δ42*fmt* strain harboring vector or $pCAT_{am1}metY_{CUA/3GC}$, respectively. Lane 5/bar 5 and lane 6/bar 6 show KL16fmt_{am274} without or with $pCAT_{am1}metY_{CUA/3GC}$. Lane 7/bar 7 show KL16fmt_{am274} with $pCAT_{am1}metY_{CUA/3GC}$ but where the *fmt* gene was not 3X FLAG tagged. (**B**, i) Formylation activity in B2 was also assayed by the northern blotting of *in vitro* reactions. Lane 1 shows deacylated i-tRNA used for *in vitro* aminoacylation with *E. coli* MetRS (lanes 2 and 8). The aminoacylated i-tRNA was incubated for different times as indicated with total cell protein prepared from either KL16 (lanes 2–7) or KL16fmt_{am274} (lanes 8–13) strains containing the $i\text{-}tRNA_{CUA/3GC}$ (total cell protein used for KL16fmt_{am274} and KL16 were 80 µg and 8 µg, respectively). (**B**, ii) Rate of formylation as quantified from the northern blotting of *in vitro* reactions.

steps of initiation and elongation because of its low efficiency of formylation (at the population level). To further validate the participation of $i\text{-}tRNA_{CUA/3GC}$ at the steps of initiation and elongation, we made use of the CA274 strain with an amber mutation in the ORF of its β-galactosidase gene (*lacZ125*), and its derivative harboring fmt_{am274}:*kan* allele; and introduced in them $pCAT_{am1}metY_{CUA/3GC}$. For assessment of the initiation using CAT_{am1} reporter, the strains were streaked on Cm containing plates (Figure 5A). The fmt_{am274}:*kan* allele resulted in Cm^R (Figure 5A, compare sectors 1 and 3). Introduction of *fmt* on a compatible plasmid resulted in loss of the Cm^R (Figure 5A, compare sectors 3 and 4). The parent CA274 strain with and without Fmt overproduction grew only on Amp (Figure 5A, sectors 1 and 2). The CAT activity assays validated the plate assays (Figure 5B).

For assessment of the elongation activity of $i\text{-}tRNA_{CUA/3GC}$, β-galactosidase (LacZ) expression was monitored. In this assay, a strain (CA275) isogenic to CA274 was also used. In CA275, the presence of a suppressor tRNA [tyrT66 (AS)] allows read through of the amber codon in the *lacZ125* ORF and serves as a positive control (Figure 5C). When grown on MacConkey agar plate, CA275 results in pink colonies (Lac^+). However, CA274 (lacking a suppressor tRNA) is seen as white/colorless colonies (Lac^-). Introduction of empty vector or $pCAT_{am1}metY_{CUA/3GC}$ in CA275 leaves its Lac^+ phenotype unchanged (Figure 5C, sectors 1–4). The CA274 showed Lac^- phenotype upon introduction of empty vector or $pCAT_{am1}metY_{CUA/3GC}$(Figure 5C, sectors 5–8), suggesting that the $i\text{-}tRNA_{CUA/3GC}$ does not lead to production of LacZ. However, while the CA274fmt_{am274} strain showed a Lac^- phenotype with the empty vector (Figure 5C, sector 9), it showed a weak Lac^+ phenotype upon introduction of $pCAT_{am1}metY_{CUA/3GC}$, which gradually led to a clearly visible Lac^+ phenotype upon longer incubation (Figure 5C, compare sector 11 at 20 h and 32 h) suggesting that when the $i\text{-}tRNA_{CUA/3GC}$ population is not rapidly formylated, it does participate at the step of elongation to suppress the amber codon not only in fmt_{am274} but also in *lacZ125* in CA274. Quantification of LacZ activities (Figure 5D) showed that the CA275 strain produced 80–100 miller units independent of the presence or absence of $i\text{-}tRNA_{CUA/3GC}$ and the activity produced by the CA274 strain was undetectable. CA274fmt_{am274} produced 25–30 miller units only in the presence of $i\text{-}tRNA_{CUA/3GC}$, and overexpression of Fmt (from p*fmt*) in this strain abolished this activity (Figure 5C and D, compare sectors/bars 11 and 12). To ensure that the elongation activity of $i\text{-}tRNA_{CUA/3GC}$, was not a context dependent phenomenon in *lacZ125*, we used yet another reporter plasmid $pCAT_{am27}metY_{CUA/3GC}$ harboring CAT gene with AUG start codon but an amber stop codon in its ORF at 27th position. The plasmid confers Cm resistance only if the amber codon at the 27th

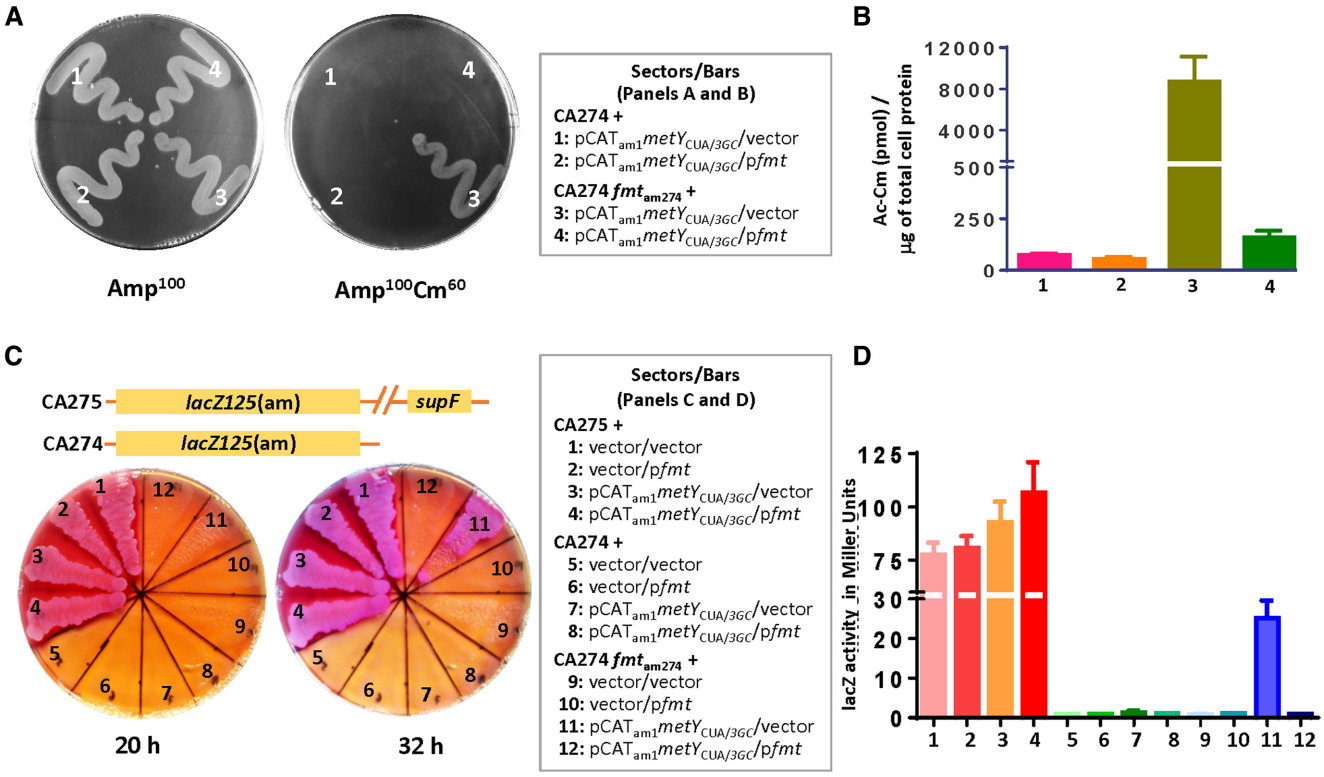

Figure 5. Participation of i-tRNA$_{CUA/3GC}$ at the steps of initiation and elongation. (**A**) Growth of indicated *E. coli* strains at 37°C on LB agar plate containing (i) Amp 100 μg/ml; (ii) Amp 100 μg/ml and Cm 60 μg/ml as indicated. Overnight cultures of *E. coli* CA274/pCAT$_{am1}$*metY*$_{CUA/3GC}$ or its derivative CA274*fmt*$_{am274}$/pCAT$_{am1}$*metY*$_{CUA/3GC}$ containing vector (sectors 1, 3) or p*fmt* (sectors 2, 4), respectively were streaked and incubated at 37°C for ∼18 h. (**B**) Initiation activity of CA274 harboring vector (lane 1) or p*fmt* (lane 2) and CA274*fmt*$_{am274}$ harboring vector (lane 3) or p*fmt* (lane 4), along with i-tRNA$_{CUA/3GC}$. (**C**) Growth of *E. coli* strains at 37°C on MacConkey agar as indicated at two time points. CA275 (LacZ$^+$) (sectors 1–4); CA274 (LacZ$^-$) (sectors 5–8); CA274*fmt*$_{am274}$ (sectors 9–10) with vectors or p*fmt*. CA274*fmt*$_{am274}$ harboring pCAT$_{am1}$*metY*$_{CUA/3GC}$ (sectors 11) and CA274*fmt*$_{am274}$ harboring pCAT$_{am1}$*metY*$_{CUA/3GC}$ and p*fmt* (sector 12). (**D**) Elongation activity of i-tRNA$_{CUA/3GC}$ in *E. coli* strains measured as read through of *lacZ125* to produce β-galactosidase. Cell extracts for both initiation and elongation activity were made from log phase ∼0.6 OD$_{600\ nm}$ cultures.

position is read through. As seen in Supplementary Figure S6, the construct conferred Cm resistance to KL16*fmt*$_{am274}$ strain (sectors 3 and 4) but not in the parent KL16 strain (sectors 1 and 2). Taken together, these observations suggest that, if not swiftly formylated, the i-tRNA (at least the i-tRNA$_{CUA/3GC}$) could function both at the initiation and the elongation steps.

Efficiency of formylation of i-tRNA population determines its distribution between IF2 and EF-Tu

For participation in protein synthesis, i-tRNA binds to IF2, and the formylated form of the i-tRNA is its preferred substrate (9,29,30). In contrast, elongator tRNAs bind to EF-Tu. As the i-tRNA$_{CUA/3GC}$ showed activities both as an initiator and an elongator under the conditions of low efficiency of formylation of i-tRNA population, we investigated for its interaction with IF2 and EF-Tu. Interestingly, we observed ∼5 fold increase in the binding of i-tRNA$_{CUA/3GC}$ to EF-Tu in the KL16*fmt*$_{am274}$ strain when compared to the wild type strain (Figure 6A, compare lane/bar 1 with 2) suggesting that availability of unformylated i-tRNA, even though it has a mismatch at the 1 × 72 position, allows its binding to EF-Tu (and its participation at the step of elongation). As a control, IF2 pull down experiments showed that i-tRNA$_{CUA/3GC}$ bound efficiently to IF2 independent of the strain used (Figure 6B, compare lane/bar 1 with 2). Furthermore, overexpression of IF2 in CA274*fmt*$_{am274}$ sequestered i-tRNA$_{CUA/3GC}$ into initiation pathway and made it unavailable for elongation (Supplementary Figure S7, compare sectors 3 and 4, 30 h).

DISCUSSION

During translation initiation, the two highly conserved features of i-tRNA, formylation and the presence of the 3GC pairs in the anticodon stem are crucial for its binding to the ribosomal P-site. Recently, we showed that a major role of the formylation is in initial targeting of the i-tRNA to the 30S ribosome, and that of the 3GC pairs in facilitating i-tRNA transitions from 30S to 70S IC, and then to elongation-competent 70S by release of IF3 (2). The presence of C1xA72 mismatch in *E. coli* i-tRNAs also contributes to its participation in initiation by avoiding its binding to EF-Tu (12,31,32). Although, our observations in this study suggest that the 1 × 72 mismatch alone does not fully abolish binding of the aminoacylated-i-tRNA to EF-Tu, it must also be formylated. Occurrence of multiple copies of the i-tRNA genes (four in *E. coli*) to produce optimal cellular levels of i-tRNA, is another factor that contributes to the

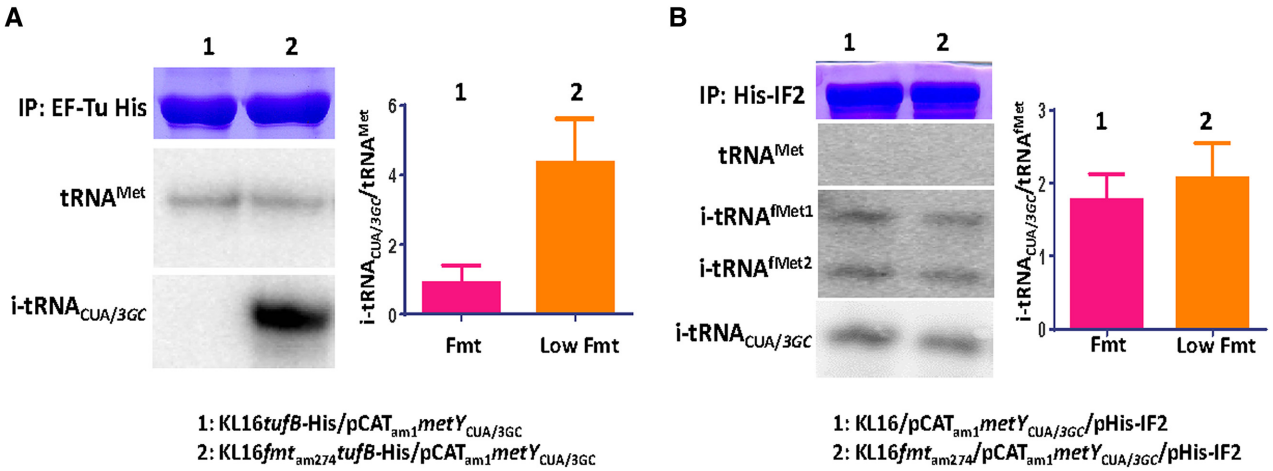

Figure 6. Binding of i-tRNA$_{CUA/3GC}$ to EF-Tu and IF2. (**A**) EF-Tu pull down was performed using *E. coli* KL16 (lane 1) and KL16*fmt*$_{am274}$ (lane 2) strains His-tagged at the C-terminal of EF-Tu (*tuf*B genes) by standard genetic techniques. EF-Tu was pulled down using Ni-NTA beads and analyzed for EF-Tu by SDS-PAGE and for tRNAs by northern blotting using specific probes. (**B**) IF2 pull down was performed from KL16 (lane 1) and KL16*fmt*$_{am274}$ (lane 2) strains. His-tagged IF2 was overexpressed in both the strains and pulled down using Ni-NTA beads and analyzed by SDS-PAGE and northern blotting for IF2 and i-tRNA, respectively. The blot was also probed for wild type i-tRNA as positive control and elongator tRNA^{Met} as negative control.

fidelity of i-tRNA selection on the ribosomes. Earlier, while characterizing the D4 and D27 suppressor strains (isolated in the same genetic screen), we showed that down regulation of expression of i-tRNAs from the *metZWV* locus (housing three of the four i-tRNA genes in *E. coli*) allowed initiation with the i-tRNA$_{CUA/3GC}$ as also with the elongator tRNAs (20,33).

To this coterie of i-tRNA traits that ensures fidelity of initiation with i-tRNA, we add one more. In this study, we have uncovered that not just the formylation of i-tRNA (e.g. in B2, i-tRNA accumulates predominantly in the formylated state) but also the kinetics of formylation of the cellular i-tRNA pools is crucial for its ability to mount a potent competition against the non-initiator tRNAs for their binding to the ribosomal P-site, and avoiding initiation by them. As the levels of Fmt are lowered, initiation with the plasmid borne i-tRNA$_{CUA/3GC}$ (a tRNA lacking the highly conserved feature of the 3GC pairs) is allowed, suggesting that under these conditions, the competition from the chromosomally encoded i-tRNA, which effectively excluded i-tRNA$_{CUA/3GC}$ from initiating under the conditions of wild type levels of Fmt, is compromised. However, given that both i-tRNA and i-tRNA$_{CUA/3GC}$ are proficient substrates for Fmt, how does a lower efficiency of formylation in B2 allow i-tRNA$_{CUA/3GC}$ to initiate? We earlier showed that the relative levels of i-tRNA and i-tRNA$_{CUA/3GC}$ are important in allowing initiation with the latter. For example, when the i-tRNA$_{CUA/3GC}$ was overexpressed from two plasmids in the wild type KL16 parent, we could detect initiation with the i-tRNA$_{CUA/3GC}$ even when all four copies of the chromosomally encoded i-tRNAs were intact (20). In B2, this imbalance (in the favour of i-tRNA$_{CUA/3GC}$) is reached through an indirect network. The existing levels of i-tRNA$_{CUA/3GC}$ are important (for its transiently available unformylated form to participate in elongation to suppress the *fmt*$_{am274}$) to produce just the adequate levels of Fmt, which in turn regulates the formylation of the cellular i-tRNA population such that the available fraction of formylated i-tRNA$_{CUA/3GC}$ is now adequate to face lesser of competition from the chromosomally encoded i-tRNAs (due to decreased availability of its formylated form at a given time). Such an equilibrium between the formylated fractions of i-tRNA and i-tRNA$_{CUA/3GC}$ allows the later to initiate from the CAT$_{am1}$ reporter used in our genetic screen. Interestingly, when we tilted the equilibrium in favour of the wild type i-tRNA by its overproduction in B2, initiation by i-tRNA$_{CUA/3GC}$ decreased (Supplementary Figure S8). In fact, unlike the other suppressors that we characterised so far (19–21), we were unable to cure off the original pCAT$_{am1}$*metY*$_{CUA/3GC}$ plasmid from B2. In retrospect, it is readily understandable. Any cells of the B2 strain devoid of the pCAT$_{am1}$*metY*$_{CUA/3GC}$ plasmid would lack Fmt, resulting in a severe growth retardation, and failure to outcompete the plasmid containing population of cells.

More importantly, what our genetic analyses are revealing is that there are multiple strategies (e. g. the number of i-tRNA genes, formylation, the presence of the 3GC pairs) the cell employs to achieve preferential initiation with an authentic i-tRNA. Any imbalances (deficiencies) in these, disturb the cellular network to now allow even the non-initiator tRNAs (including, as we have shown earlier, genuine elongator tRNAs) to initiate. Is such a phenomenon physiologically relevant? While fidelity of any cellular processes is important for its long term sustenance, regulated levels of 'leakages' or 'plasticity' in fidelity are also desirable traits, important for the cells to evolve (with changes in the genotype), or to cope with the varying environmental conditions (without a genotypic change). For example, it is known that (p)ppGpp levels regulate transcription from *metZWV* (34). And, the *metY* gene may also be regulated in response to arginine metabolism (35). Decreases in cellular levels of i-tRNA (under various stressful conditions) may not only lead to leakages in the fidelity of initiation but may also regulate ribosome biogenesis (36) and in generating ribosomal heterogeneity of the kind important in translation of select mRNAs (37,38). Regulation of initi-

ation by changes in i-tRNA gene copy number is also a known phenomenon for the fitness of *E. coli* under different nutrient conditions (39). Also, even though *fmt* is crucial for the normal growth of *E. coli* it is not essential for its vitality. The Δ*fmt* strains, as shown in this study and also reported earlier, are viable. However, they grow poorly (10) but the growth defect can be rescued by overexpression of i-tRNA. Interestingly, in Salmonella, resistance to Fmt inhibitors arose by amplifications of the tandemly repeated *metZ*, *metW* and *metV* genes, encoding i-tRNA (40).

While in the B2 suppressor, the kinetics of formylation is affected by a mutation (requiring read through) in *fmt*, this could also occur independent of the genetic change. The formylation reaction requires availability of 10-formyl-THF, produced by the one-carbon metabolic pathway. Thus, nutritional changes in which *E. coli* grows could also regulate the rate of formylation by regulating production of 10-formyl-THF. Modulation of translation initiation by regulating formylase levels (by governing the fidelity of initiation) appears yet another paradigm for alternative translation mechanisms. Thus, conditions which hamper formylation might enhance initiation with certain elongator tRNAs from non-canonical sites and synthesise new peptides which might act as regulators of stress signalling. Recently, changes in the aminoacylation status of tRNAs have been shown to result in gain of phenotypic resistance/tolerance against antibiotics without a genotypic change (41).

Our observations with B2 also provide a basis for the use of single $tRNA^{Met}$ in mammalian mitochondria at both the steps of initiation and elongation. Incomplete formylation of this tRNA is thought to be the mechanism for the dual function of the mitochondrial $tRNA^{Met}$ (42,43). Our observations that the $i\text{-}tRNA_{CUA/3GC}$ participates both at the steps of initiation and elongation in the fmt_{am274} strain provide experimental support to the model.

Finally, the genetic screen that we set up (19) is unravelling important aspects of how *E. coli* ensures accuracy of selection of i-tRNA in the P-site. A rapid rate of formylation would seem as an obvious way of ensuring fidelity of i-tRNA binding to the P-site (and excluding all others from binding), to predict this from the kinetic parameters (e.g. K_m and V_{max} etc.) of formylation of the wild type i-tRNA with the wild type Fmt would have not been obvious. We believe the analysis we present here, highlights yet again the enormous regulation the biological systems employ by fine tuning the levels of various cellular proteins and the metabolites, to retain growth fitness advantage in different ecological niches.

SUPPLEMENTARY DATA

Supplementary Data are available at NAR Online.

ACKNOWLEDGEMENTS

We thank our laboratory colleagues for their suggestions on the manuscript.

FUNDING

Department of Science and Technology (DST) and Department of Biotechnology (DBT), New Delhi, India; DBT-IISc partnership programme, University Grants Commission, New Delhi for the Centre of Advanced Studies, and the DST-FIST level II infrastructure supports to carry out this work. U.V. is a J.C. Bose fellow of the DST, New Delhi, India. R.A.S., S.S., S.S. and K.L. received various fellowships from the Council of Scientific and Industrial Research, New Delhi. Funding for open access charge: From the research funds to the corresponding author.
Conflict of interest statement. None declared.

REFERENCES

1. Gold,L. (1988) Posttranscriptional regulatory mechanisms in Escherichia coli. *Annu. Rev. Biochem.*, **57**, 199–233.
2. Shetty,S., Shah,R.A., Chembazhi,U.V., Sah,S. and Varshney,U. (2017) Two highly conserved features of bacterial initiator tRNAs license them to pass through distinct checkpoints in translation initiation. *Nucleic Acids Res.*, **45**, 2040–2050.
3. Guillon,J.M., Meinnel,T., Mechulam,Y., Lazennec,C., Blanquet,S. and Fayat,G. (1992) Nucleotides of tRNA governing the specificity of Escherichia coli methionyl-tRNA(fMet) formyltransferase. *J. Mol. Biol.*, **224**, 359–367.
4. Lee,C.P., Seong,B.L. and RajBhandary,U.L. (1991) Structural and sequence elements important for recognition of Escherichia coli formylmethionine tRNA by methionyl-tRNA transformylase are clustered in the acceptor stem. *J. Biol. Chem.*, **266**, 18012–18017.
5. Schmitt,E., Blanquet,S. and Mechulam,Y. (1996) Structure of crystalline Escherichia coli methionyl-tRNA(f)Met formyltransferase: comparison with glycinamide ribonucleotide formyltransferase. *EMBO J.*, **15**, 4749–4758.
6. Gite,S., Li,Y., Ramesh,V. and RajBhandary,U.L. (2000) Escherichia coli methionyl-tRNA formyltransferase: role of amino acids conserved in the linker region and in the C-terminal domain on the specific recognition of the initiator tRNA. *Biochemistry*, **39**, 2218–2226.
7. Gite,S. and RajBhandary,U.L. (1997) Lysine 207 as the site of cross-linking between the 3′-end of Escherichia coli initiator tRNA and methionyl-tRNA formyltransferase. *J. Biol. Chem.*, **272**, 5305–5312.
8. Ramesh,V., Gite,S. and RajBhandary,U.L. (1998) Functional interaction of an arginine conserved in the sixteen amino acid insertion module of Escherichia coli methionyl-tRNA formyltransferase with determinants for formylation in the initiator tRNA. *Biochemistry*, **37**, 15925–15932.
9. Sundari,R.M., Stringer,E.A., Schulman,L.H. and Maitra,U. (1976) Interaction of bacterial initiation factor 2 with initiator tRNA. *J. Biol. Chem.*, **251**, 3338–3345.
10. Guillon,J.M., Mechulam,Y., Schmitter,J.M., Blanquet,S. and Fayat,G. (1992) Disruption of the gene for Met-tRNA(fMet) formyltransferase severely impairs growth of Escherichia coli. *J. Bacteriol.*, **174**, 4294–4301.
11. Majumdar,A., Bose,K.K. and Gupta,N.K. (1976) Specific binding of Excherichia coli chain Initiation factor 2 to fMet-tRnafMet. *J. Biol. Chem.*, **251**, 137–140.
12. Guillon,J.M., Heiss,S., Soutourina,J., Mechulam,Y., Laalami,S., Grunberg-Manago,M. and Blanquet,S. (1996) Interplay of methionine tRNAs with translation elongation factor Tu and translation initiation factor 2 in Escherichia coli. *J. Biol. Chem.*, **271**, 22321–22325.
13. Varshney,U., Lee,C.P., Seong,B.L. and RajBhandary,U.L. (1991) Mutants of initiator tRNA that function both as initiators and elongators. *J. Biol. Chem.*, **266**, 18018–18024.
14. Schulman,L.H. and Pelka,H. (1975) The structural basis for the resistance of Escherichia coli formylmethionyl transfer ribonucleic acid to cleavage by Escherichia coli peptidyl transfer ribonucleic acid hydrolase. *J. Biol. Chem.*, **250**, 542–547.

15. Kossel,H. and RajBhandary,U.L. (1968) Studies on polynucleotides. LXXXVI. Enzymic hydrolysis of N-acylaminoacyl-transfer RNA. *J. Mol. Biol.*, **35**, 539–560.
16. Atherly,A.G. and Menninger,J.R. (1972) Mutant E. coli strain with temperature sensitive peptidyl-transfer RNA hydrolase. *Nature: New Biol.*, **240**, 245–246.
17. Varshney,U. and RajBhandary,U.L. (1990) Initiation of protein synthesis from a termination codon. *PNAS*, **87**, 1586–1590.
18. Mandal,N., Mangroo,D., Dalluge,J.J., McCloskey,J.A. and Rajbhandary,U.L. (1996) Role of the three consecutive G:C base pairs conserved in the anticodon stem of initiator tRNAs in initiation of protein synthesis in Escherichia coli. *RNA*, **2**, 473–482.
19. Das,G., Thotala,D.K., Kapoor,S., Karunanithi,S., Thakur,S.S., Singh,N.S. and Varshney,U. (2008) Role of 16S ribosomal RNA methylations in translation initiation in Escherichia coli. *EMBO J.*, **27**, 840–851.
20. Kapoor,S., Das,G. and Varshney,U. (2011) Crucial contribution of the multiple copies of the initiator tRNA genes in the fidelity of tRNA(fMet) selection on the ribosomal P-site in Escherichia coli. *Nucleic Acids Res.*, **39**, 202–212.
21. Shetty,S., Nadimpalli,H., Shah,R.A., Arora,S., Das,G. and Varshney,U. (2014) An extended Shine-Dalgarno sequence in mRNA functionally bypasses a vital defect in initiator tRNA. *PNAS*, **111**, E4224–E4233.
22. Seshadri,A., Dubey,B., Weber,M.H. and Varshney,U. (2009) Impact of rRNA methylations on ribosome recycling and fidelity of initiation in Escherichia coli. *Mol. Microbiol.*, **72**, 795–808.
23. Datsenko,K.A. and Wanner,B.L. (2000) One-step inactivation of chromosomal genes in Escherichia coli K-12 using PCR products. *PNAS*, **97**, 6640–6645.
24. Uzzau,S., Figueroa-Bossi,N., Rubino,S. and Bossi,L. (2001) Epitope tagging of chromosomal genes in Salmonella. *PNAS*, **98**, 15264–15269.
25. Sarin,P.S. and Zamecnik,P.C. (1964) On the stability of Aminoacyl-S-Rna to nucleophilic catalysis. *Biochim. Biophys. Acta*, **91**, 653–655.
26. Schofield,P. and Zamecnik,P.C. (1968) Cupric ion catalysis in hydrolysis of aminoacyl-tRNA. *Biochim. Biophys. Acta*, **155**, 410–416.
27. Bradford,M.M. (1976) A rapid and sensitive method for the quantitation of microgram quantities of protein utilizing the principle of protein-dye binding. *Anal. Biochem.*, **72**, 248–254.
28. Miller,J.H. (1972) *Experiments in Molecular Genetics*. Cold Spring Harbour, NY.
29. Hartz,D., McPheeters,D.S. and Gold,L. (1989) Selection of the initiator tRNA by Escherichia coli initiation factors. *Genes Dev.*, **3**, 1899–1912.
30. Petersen,H.U., Roll,T., Grunberg-Manago,M. and Clark,B.F. (1979) Specific interaction of initiation factor IF2 of E. coli with formylmethionyl-tRNA f Met. *Biochem. Biophys. Res. Commun.*, **91**, 1068–1074.
31. Seong,B.L. and RajBhandary,U.L. (1987) Mutants of Escherichia coli formylmethionine tRNA: a single base change enables initiator tRNA to act as an elongator in vitro. *PNAS*, **84**, 8859–8863.
32. Guillon,J.M., Mechulam,Y., Blanquet,S. and Fayat,G. (1993) Importance of formylability and anticodon stem sequence to give a tRNA(Met) an initiator identity in Escherichia coli. *J. Bacteriol.*, **175**, 4507–4514.
33. Samhita,L., Virumae,K., Remme,J. and Varshney,U. (2013) Initiation with elongator tRNAs. *J. Bacteriol.*, **195**, 4202–4209.
34. Nagase,T., Ishii,S. and Imamoto,F. (1988) Differential transcriptional control of the two tRNA(fMet) genes of Escherichia coli K-12. *Gene*, **67**, 49–57.
35. Krin,E., Laurent-Winter,C., Bertin,P.N., Danchin,A. and Kolb,A. (2003) Transcription regulation coupling of the divergent argG and metY promoters in Escherichia coli K-12. *J. Bacteriol.*, **185**, 3139–3146.
36. Shetty,S. and Varshney,U. (2016) An evolutionarily conserved element in initiator tRNAs prompts ultimate steps in ribosome maturation. *PNAS*, **113**, E6126–E6134.
37. Temmel,H., Muller,C., Sauert,M., Vesper,O., Reiss,A., Popow,J., Martinez,J. and Moll,I. (2017) The RNA ligase RtcB reverses MazF-induced ribosome heterogeneity in Escherichia coli. *Nucleic Acids Res.*, **45**, 4708–4721.
38. Vesper,O., Amitai,S., Belitsky,M., Byrgazov,K., Kaberdina,A.C., Engelberg-Kulka,H. and Moll,I. (2011) Selective translation of leaderless mRNAs by specialized ribosomes generated by MazF in Escherichia coli. *Cell*, **147**, 147–157.
39. Samhita,L., Nanjundiah,V. and Varshney,U. (2014) How many initiator tRNA genes does Escherichia coli need? *J. Bacteriol.*, **196**, 2607–2615.
40. Nilsson,A.I., Zorzet,A., Kanth,A., Dahlstrom,S., Berg,O.G. and Andersson,D.I. (2006) Reducing the fitness cost of antibiotic resistance by amplification of initiator tRNA genes. *PNAS*, **103**, 6976–6981.
41. Javid,B., Sorrentino,F., Toosky,M., Zheng,W., Pinkham,J.T., Jain,N., Pan,M., Deighan,P. and Rubin,E.J. (2014) Mycobacterial mistranslation is necessary and sufficient for rifampicin phenotypic resistance. *PNAS*, **111**, 1132–1137.
42. Takeuchi,N., Kawakami,M., Omori,A., Ueda,T., Spremulli,L.L. and Watanabe,K. (1998) Mammalian mitochondrial methionyl-tRNA transformylase from bovine liver. Purification, characterization, and gene structure. *J. Biol. Chem.*, **273**, 15085–15090.
43. Takeuchi,N., Vial,L., Panvert,M., Schmitt,E., Watanabe,K., Mechulam,Y. and Blanquet,S. (2001) Recognition of tRNAs by Methionyl-tRNA transformylase from mammalian mitochondria. *J. Biol. Chem.*, **276**, 20064–20068.